PB88-159769

Wind Tunnel Study of the Flow Structrue and Dispersion from Sources Upwind of Three-Dimensional Hills

(U.S.) Environmental Protection Agency
Research Triangle Park, NC

1987

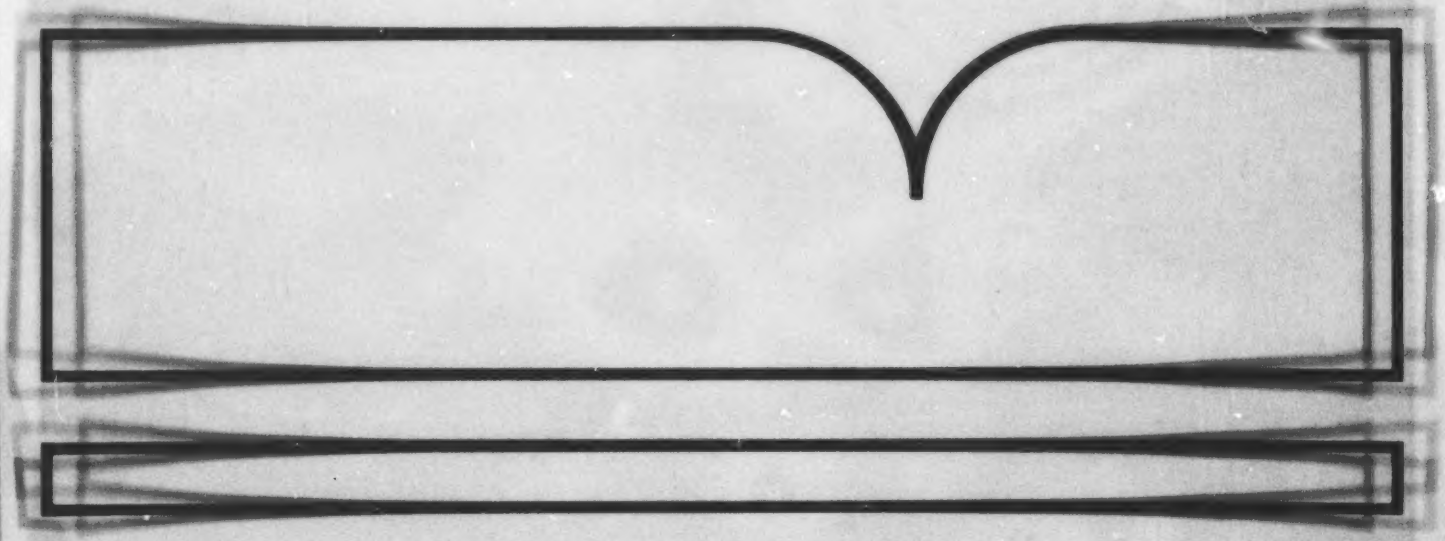

U.S. Department of Commerce
National Technical Information Service

TECHNICAL REPORT DATA
(Please read Instructions on the reverse before completing)

1. REPORT NO.	2.	3. RECIPIENT'S ACCESSION NO.
EPA/600/J-87/175		PB88-159769

4. TITLE AND SUBTITLE	5. REPORT DATE
A WIND TUNNEL STUDY OF THE FLOW STRUCTURE AND DISPERSION FROM SOURCES UPWIND OF THREE DIMENSIONAL HILLS (Journal Version)	1987
	6. PERFORMING ORGANIZATION CODE

7. AUTHOR(S)	8. PERFORMING ORGANIZATION REPORT NO.
William H. Snyder[1] R.E. Britter[2]	

9. PERFORMING ORGANIZATION NAME AND ADDRESS	10. PROGRAM ELEMENT NO.
Atmospheric Sciences Research Laboratory Office of Research and Development U.S. Environmental Protection Agency Research Triangle Park, NC 27711	CDTA1D/02 - 1313 (FY-85)
	11. CONTRACT/GRANT NO.

12. SPONSORING AGENCY NAME AND ADDRESS	13. TYPE OF REPORT AND PERIOD COVERED
Atmospheric Sciences Research Laboratory - RTP, NC Office of Research and Development U.S. Environmental Protection Agency Research Triangle Park, NC 27711	
	14. SPONSORING AGENCY CODE EPA/600/09

15. SUPPLEMENTARY NOTES Atmospheric Environment, 21(4):735-751, April 1987
1. On assignment from the National Oceanic Atmospheric Association, U.S. Dept. of Commerce.
2. Department of Engineering, University of Cambridge, Cambridge, U.K.

16. ABSTRACT

The flow fields around moderately steep hills of triangular cross section and varying crosswind aspect ratio and around a bell-shaped hill were examined by using models immersed in a simulated neutral atmospheric boundary layer in a meteorological wind tunnel. The triangular hills ranged from an axisymmetric cone to a two-dimensional (2-D) ridge. Concentration patterns resulting from sources of three heights placed upwind of each of these hills were examined to determine plume deformations and terrain amplification factors. Plumes from elevated sources approached the hill surfaces much more closely the smaller the aspect ratio; streamline displacements were generally within the limits suggested by potential flow theory. The terrain amplification factor A, defined as the ratio of the maximum surface concentration in the presence of the hill to the maximum in flat terrain, was found to decrease with increasing aspect ratio. For the half-hill-height sources, values of A ranged from 4 for the bell-shaped hill down to 1.5 for the 2-D ridge; for the hill-height source, from 1.8 for the cone down to 0.6 for the 2-D ridge. The latter value is suspect, however, because larger concentrations are expected downwind of the reattachment point, a region not probed in the current study.

17. KEY WORDS AND DOCUMENT ANALYSIS

a. DESCRIPTORS	b. IDENTIFIERS/OPEN ENDED TERMS	c. COSATI Field/Group

18. DISTRIBUTION STATEMENT	19. SECURITY CLASS (This Report)	21. NO. OF PAGES
RELEASE TO PUBLIC	UNCLASSIFIED	19
	20. SECURITY CLASS (This page)	22. PRICE
	UNCLASSIFIED	MF PC 12.95/$6.95

EPA Form 2220-1 (Rev. 4-77) PREVIO...

REPRODUCED BY
U.S. DEPARTMENT OF COMMERCE
NATIONAL TECHNICAL
INFORMATION SERVICE
SPRINGFIELD, VA. 22161

EPA/600/J-87/175
JOURNAL ARTICLE

Atmospheric Environment Vol. 21, No. 4, pp. 735–751, 1987.
Printed in Great Britain.

0004–6981/87 $3.00 + 0.00
Pergamon Journals Ltd.

A WIND TUNNEL STUDY OF THE FLOW STRUCTURE AND DISPERSION FROM SOURCES UPWIND OF THREE-DIMENSIONAL HILLS

WILLIAM H. SNYDER*
Meteorology & Assessment Division, Atmospheric Sciences Research Laboratory, U.S. Environmental Protection Agency, Research Triangle Park, NC 27711, U.S.A.

and

R. E. BRITTER
Department of Engineering, University of Cambridge, Cambridge CB2 1PZ, U.K.

(*First received* 22 *July* 1985 *and in final form* 9 *June* 1986)

Abstract—The flow fields around moderately steep hills of triangular cross section and varying crosswind aspect ratio and around a bell-shaped hill were examined by using models immersed in a simulated neutral atmospheric boundary layer in a meteorological wind tunnel. The triangular hills ranged from an axisymmetric cone to a two-dimensional ridge. Concentration patterns resulting from sources of three heights placed upwind of each of these hills were examined to determine plume deformations and terrain amplification factors. The separated flow fields, increasing in size with increasing aspect ratio, appeared to have dominating influences on the entire flow structure; changes in several flow parameters were plausibly explained in terms of the notion that the effective hill shape was the hill-plus-recirculation region rather than the actual hill shape. The concentration measurements showed strong distortions of plume shapes effected by the hills, with convergence in vertical planes and divergence in horizontal planes. Plumes from elevated sources approached the hill surfaces much more closely the smaller the aspect ratio; streamline displacements were generally within the limits suggested by potential flow theory. The terrain amplification factor A, defined as the ratio of the maximum surface concentration in the presence of the hill to the maximum in flat terrain, was found to decrease with increasing aspect ratio. For the half-hill-height sources, values of A ranged from 4 for the bell-shaped hill down to 1.5 for the two-dimensional ridge; for the hill-height source, from 1.8 for the cone down to 0.6 for the two-dimensional ridge. The latter value is suspect, however, because larger concentrations are expected downwind of the reattachment point, a region not probed in the current study.

Key word index: Atmospheric diffusion, complex terrain, wind-tunnel modeling, air pollution, atmospheric boundary layer.

1. INTRODUCTION

Most of the current practical mathematical models that attempt to predict pollutant concentrations in complex terrain ignore the complexity of the terrain. They typically use Gaussian diffusion in conjunction with a simple terrain adjustment factor such as the half-height formula (which is completely independent of hill shape) to estimate the closeness of approach of the plume centerline to the hill surface. The deformation of the flow field by a hill will, by itself, have no effect on the ground-level concentration. However, when diffusive mixing is also considered, the closeness of approach of the plume centerline (i.e. the deformation) becomes an extremely important factor in the estimation of ground-level concentrations. The approach distance is known to be strongly dependent upon the shape of the hill. As an example, potential-flow theory suggests that the streamline originating far upwind of a half-cylinder hill at half the hill height h passes the crest at a distance of 0.28 h from the surface, whereas for a hemispherical hill, it passes the crest at a distance of 0.08 h. Such large differences in approach distances can result in *very* large differences in estimated surface concentrations. These two cases (two-dimensional and axisymmetric) would appear to bracket the extremes to be expected in the real world, but because of the large differences in the two extremes, further information is needed to allow interpolation between them.

The objective of this study was to gain understanding of the flow structure around two- and three-dimensional hills immersed in a simulated neutral atmospheric boundary layer. More specifically, it was desired to determine (1) how long (acrosswind) a hill must be to be considered as two-dimensional rather than three-dimensional, (2) how closely a plume from an upwind source would approach the hill surface as a function of the hill's aspect ratio, and (3) the locations and values of the maximum surface concentrations.

To achieve these goals, mean and turbulent velocity measurements were made upwind and near the hills

*On assignment from the National Oceanic and Atmospheric Administration, U.S. Department of Commerce.

NTIS is authorized to reproduce and sell this report. Permission for further reproduction must be obtained from the copyright owner.

together with the characteristics of plumes from upwind sources. The velocity measurements are helpful in interpreting the concentration results; further, data sets containing both velocity *and* concentration measurements are essential for development and testing of numerical and analytical models of diffusion in complex terrain. For example, a useful analytical model of diffusion in complex terrain (Hunt *et al.*, 1979) relies upon knowledge of the path of the streamline through the source and the turbulence encountered by the plume following that streamline.

A previous paper (Snyder and Hunt, 1984) presented measurements of plumes being transported over a bell-shaped hill where the approach flow was neutral and of essentially uniform velocity (thin boundary layer) and low turbulence intensity. Similar measurements were made in the present study around the bell-shaped hill to examine the effect of a deep boundary layer on the flow structure over the hill and on the resulting surface concentrations. However, it was more convenient to extend a cone-shaped hill in order to obtain hills of various crosswind aspect ratios. Thus, the basic hill shape for the present study was a cone; larger aspect ratios were obtained by inserting straight-sided triangular sections between two halves of the basic cone.

Mean flow and turbulence profiles were measured on the centerline at the crest and at the upwind base of each of these hills. Attempts were made to obtain measurements in 'natural' coordinates, i.e. in coordinates along and perpendicular to the local mean streamlines. Ethylene (C_2H_4) tracer was released upstream of each hill at three elevations above ground: $H_s = 0$, $h/2$, and h, where H_s is the source height and h is the hill height. Various types of concentration measurements were made downstream of each source, including vertical and lateral profiles above the crests of the hills. In addition, detailed measurements were made along the surface of the bell-shaped hill so that complete maps of surface concentration patterns were obtained. Statistical measures of the various distributions were also computed. Finally, measurements of flow structure and plume dispersion were made over flat terrain for comparison with those over the various hills.

To put this study in perspective, it is useful to discuss several recent wind-tunnel studies. Britter *et al.* (1981) studied the flow structure over smooth and rough two-dimensional hills with small slopes (about 15°) immersed in a deep neutral boundary layer. Courtney (1979) made similar measurements over a hill very similar in shape and, in addition, measured diffusion patterns resulting from sources of various heights upwind of this hill. Both Britter *et al.* and Courtney found very thin, intermittently separated regions on the lee slopes of the hills. The diffusion measurements by Courtney suggested only very small effects of the hill on the surface concentration patterns (compared with those over flat terrain).

Arya *et al.* (1981) studied the influence of a very steep (63°), two-dimensional triangular ridge on the diffusion patterns from sources placed at a number of heights and positions with respect to the ridge. They found generally strong influences of the ridge, with a maximum increase in ground-level concentration (over the flat terrain value) of a factor of 10 when the source was placed within the recirculating cavity region downstream of the ridge.

Khurshudyan *et al.* (1981) collected an extensive set of data over a series of three smooth-shaped, two-dimensional hills with maximum slopes of 10°, 16° and 26°. No separation was observed on the lee side of the 10° hill. Intermittent separation was observed on the lee side of the 16° hill. A large cavity of recirculating flow was formed behind the 26° hill. With upwind sources, the maximum ground-level concentrations (*glcs*) were increased (over flat terrain values) by factors in the range of 1.1–2.5 as the slope of the hill increased. For downwind sources, maximum *glcs* increased by factors in the range of 3–15; the largest value, however, was found for a low source downwind of the 16° hill.

The current study considers three-dimensional hills with constant slopes of 26.5°, and various crosswind aspect ratios. The relatively steep slope and the discontinuity in slope at the crest insures separation at the crest, with the extent of the recirculating cavity region being dependent upon the aspect ratio. This study concentrated on the flow field at and upwind of the crest and concentration patterns resulting from sources upwind of the crest. Castro and Snyder (1982) measured the flow fields downwind of the crests and the concentration patterns resulting from sources placed downwind of these same hills. Frequent use is made of the information gained by Castro and Snyder.

Numerous other wind-tunnel studies of flow and diffusion over hills have been conducted. Only a few of those most closely related to the current objectives have been discussed.

2. EXPERIMENTAL ARRANGEMENTS

The study was conducted in the EPA Meteorological Wind Tunnel, which has a test section 3.7 m wide, 2.7 m high and 18.3 m long. It is described in detail by Snyder (1979). A nominally 1-m-thick simulated atmospheric boundary layer was obtained using a fence of height 15.3 cm placed 22.3 cm downwind of the entrance to the test section and gravel roughness (nominally 1-cm diameter gravel) covering the tunnel floor downwind of the fence. The free-stream speed was 4 m s^{-1}.

The cone (referred to as C2) had a height of 23.4 cm and a base diameter of 93.6 cm (slope of 0.5). A second cone was split in half and used as ends of the larger-aspect-ratio hills. Straight sections of length 45 cm (C4) and 90 cm (C6) were mated with the half-cone ends. Finally, an 'infinitely' long triangular ridge (CX) extended across the entire width of the test section of the tunnel. These hills are depicted in Fig. 1. The hill surfaces were not covered with gravel but were instead left smooth. The length L of the hills used in calculating

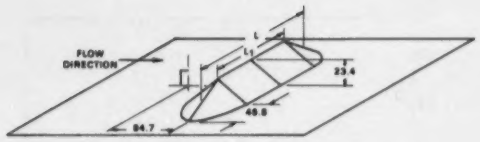

HILL	POLY	C2	C4	C6	CX
L_1, cm	–	0	46	90	∞
L, cm	48	46	91	136	∞
L/h	2.0	2.0	3.9	5.8	∞

Fig. 1. Details of hills and source. Dimensions in centimeters.

the aspect ratio is defined as the distance between the half-height points. The aspect ratio is defined as the ratio of this length to the height, and this is also shown in Fig. 1.

Another hill was also studied. It was axisymmetric, of polynomial cross section (referred to as POLY), and is described by Hunt and Snyder (1980) and Snyder and Hunt (1984). It was of roughly similar proportions to the conical hill but avoided the singularity at its peak, was flat topped, and had a maximum slope of 1.0.

The effluent (ethylene) was emitted from a 'stack' (0.635-cm OD) that was adjustable in height. It contained a 90° bend so as to avoid any cross-stream momentum in the effluent. The bent-over portion of the stack was 7 cm long.

The centers of the hills were placed 8.5 m downwind of the fence at the entrance to the test section and 84.7 cm downwind of the exit of the stack. The bases of the hills were embedded in the gravel so that an abrupt change in elevation from the tunnel floor to the bases of the hills was absent. However, because the hills were smooth, there was an abrupt change in surface roughness. Measurements of the boundary layer and the flow structure over the hills were made with hot-wire anemometry operated on-line to the facility's PDP 11/40 minicomputer (see Castro and Snyder, 1982). Corrections for varying ambient temperature and non-ideal yaw response of the hot wires were used (Lawson and Britter, 1983).

Because it was of interest to test the predictions of theoretical models (for example, rapid-distortion theory), an attempt was made to measure the flow properties in coordinates oriented along and normal to the local streamlines. The data acquisition and analysis program provided the mean flow and turbulence data, including the mean-flow angle (with respect to the probe orientation). These data were converted from probe coordinates to 'natural' coordinates so that, for example, turbulence intensities are described in directions along and normal to the local streamlines. In order to minimize errors in this conversion, three vertical profiles were obtained with the probe inclined at 0°, 10° and 20° with respect to the tunnel floor. Data for which the probe coordinate and the natural coordinate differed by more than 5° were discarded. The remaining data were converted to natural coordinates and the three profiles were then merged. In some cases this led to small discontinuities in the profiles, as the required adjustments to the data for probes not aligned with the mean flow are fairly substantial (cf. Khurshudyan *et al.*, 1981).

For the concentration measurements, high purity ethylene (C_2H_4) was used as a neutrally buoyant tracer gas. The flow rate Q was adjusted so as to maintain an isokinetic release based on the stack ID and the local mean velocity. Concentration profiles were obtained by drawing samples through flame ionization detectors with calibration, sampling and analysis procedures quite similar to those described by Castro and Snyder (1982).

Adjustments were made to the ceiling to provide a zero-pressure-gradient flow outside the boundary layer in the tunnel. This was achieved by adjusting the ceiling until the mean velocity along the tunnel centerline was constant at approximately 1.8 m above the floor of the tunnel. The magnitude of the adjustment and its extent increased with aspect ratio, no adjustment being required (above that for the base-line boundary layer) for the polynomial hill (POLY) or the cone (C2). Ceiling adjustments were made to 5 m downstream of the hill.

3. PRESENTATION AND DISCUSSION OF RESULTS

The boundary layer in the absence of the hills has been studied in some detail (Snyder and Britter, 1979) and reported briefly by Castro and Snyder (1982). At the hill position, u_*/U_∞ was 0.048 (u_* = friction velocity; U_∞ = free-stream velocity) with a roughness length z_0 of 0.13 mm. (In determining these values, the origin of the vertical coordinate z was at the tops of the roughness elements and a displacement height d of zero was found to be the most appropriate.) Concentration measurements from ground-level and elevated point and line sources in this boundary layer are available in Snyder and Britter (1979) and Khurshudyan *et al.* (1981), and their essential features have also been reported by Castro and Snyder (1982).

3.1. *Velocity measurements over the hills*

We present first the flow-field measurements made over the hills, discussing how speedup factors, mean-flow angles, turbulence intensities and Reynolds stresses change with aspect ratio. Where feasible, we make comparisons with the Jackson and Hunt (1975), Britter *et al.* (1981), and rapid-distortion theories. Where useful, we also make comparisons of the flow fields measured over the smooth- and rough-surfaced, two-dimensional ridge. We then present and briefly discuss the flow structure upwind of hills.

For each of the five hills, measurements were made with a cross-film anemometer above the crest and above the upstream base of the hill, yielding vertical profiles of mean velocity, angle of the mean flow, two components of turbulence intensity, and Reynolds stress.

3.1.1. *Hill crest.* The mean velocity profiles above the crests (Fig. 2) show significant increases in mean

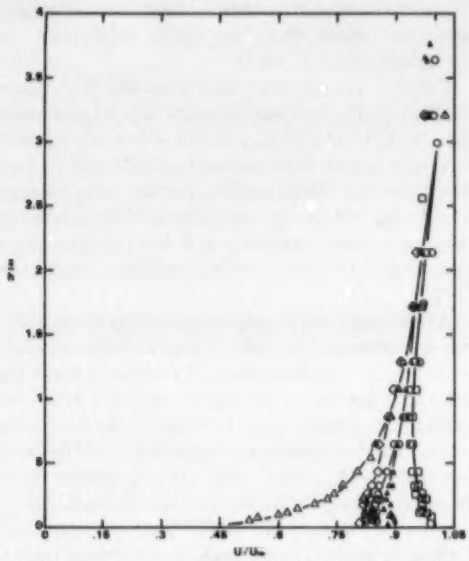

Fig. 2. Mean velocity profiles above hill crests. △, No hill; □, C2; ○, C4; ◇, C6; ▲, CX.

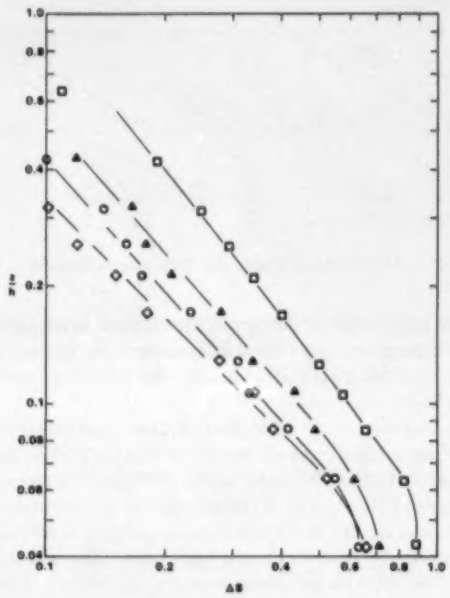

Fig. 3. Fractional speedup factors over crests of hills. □, C2; ○, C4; ◇, C6; ▲, CX.

velocity to over one hill height above the crests. Somewhat surprisingly, the profiles are very nearly uniform for about a third of the hill height above the crest. In broad terms, hills with an aspect ratio of 4 and above (C4, C6, CX) show similar flow behavior, whereas the cone (C2) is distinctly different.

A fractional speedup factor

$$\Delta S = \frac{U(z+h) - U_0(z)}{U_0(z)},$$

where $U(z+h)$ is the velocity at height z above the hill crest and $U_0(z)$ is the far upstream velocity at height z above the flat terrain, is frequently used to describe the speed-up of mean velocity over topography. This speedup factor rises to 0.9 (Fig. 3) at the lowest measuring station for the cone and to about 0.7 for C4, C6 and CX. The velocity profile for the flat-topped polynomial hill (not shown) was essentially similar to that for the cone, but velocities were a few percent larger. A slight reduction in mean velocity 5 mm (0.02 h) above the polynomial crest may have been due to separation of the flow a little upstream of the crest.

In a further experiment, the two-dimensional ridge was covered with gravel. A comparison of the velocity profiles for this ridge with and without roughness is particularly interesting (Fig. 4). The rough surface induces a slightly greater speedup over an 'outer' region above the crest, but the mean velocity is substantially reduced very near the surface (in the lowest 15 mm or 0.06 h), corresponding to the 'inner' region of Jackson and Hunt (1975) and Britter *et al.* (1981). Jackson and Hunt estimated the depth (l) of this inner region with

$$(l/z_0)\ln(l/z_0) = 2\kappa^2 L_s/z_0, \qquad (1)$$

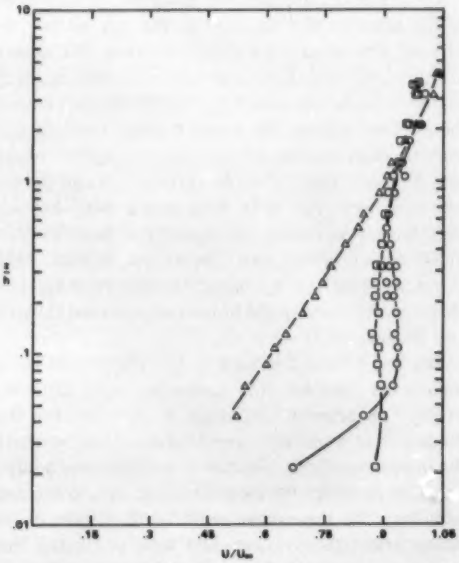

Fig. 4. Comparison of mean velocity profiles above crest of two-dimensional ridge. △, No hill; □, smooth surface, ○, gravel-covered surface.

where $\kappa = 0.4$ is von Karman's constant and L_s is the hill half-length in the streamwise direction (distance between crest and half-height point). Our estimate from (1) is $l = 15.5$ mm (0.066h). The excellent agreement between this estimate and the observed region of roughness effects is probably fortuitous, as the

Jackson–Hunt result is for slopes small compared to unity. Nevertheless, from other experiments as well, Equation (1) does seem to be a good estimator of l. The ratio $l/z_0 \simeq 119$ is larger than the $l/z_0 = 15$ obtained in the study by Britter *et al.* (1981), but the inner layer depth is still not very large compared with the size d of the individual roughness elements ($l/d \cong 1.5$). A detailed study of the structure within the inner layer will always be difficult.

Experiments with a smooth surface over the hill will produce a smaller 'inner' region [estimated by replacing z_0 by ν/u_* in Equation (1)]. The flow in the 'outer' region is independent of the structure or extent of the 'inner' region. The slight difference in velocity in the outer region evident in Fig. 4 is most probably attributable to the small changes in the separated region resulting from different separating shear layers.

The variation of ΔS with aspect ratio in Fig. 3 is far from being monotonic, being 0.82, 0.55, 0.52 and 0.61 at $z = 15$ mm (0.06 h) for C2, C4, C6 and CX, respectively. This variation persists for larger z, and it is apparent that the vertical extent of the speedup scales on L_s for all hill shapes.

The speedup factors for the different aspect-ratio hills are somewhat scattered at the higher elevations, a result, no doubt, of the subtraction of two nearly equal but uncertain measurements of velocities. The maximum speedup is of order, but smaller than, unity. Jackson and Hunt's (1975) work showed that for a bell-shaped hill $\Delta S \simeq 2(h/L_s)$ for small h/L_s and $10^{-7} \leqslant z_0/L_s \leqslant 10^{-4}$. The present experiments with $z_0/L_s = 5.5 \times 10^{-4}$ are closer to $\Delta S \simeq 1(h/L_s)$. The large value of h/L_s ($= 1$ in the present experiments) produces separation from the crests (which was observed with smoke flow visualization for C4, C6 and CX and with pulsed-wire anemometer measurements for all the hills by Castro and Snyder, 1982). At the crest position, the hill plus separated region is more of a ramp shape than a crested hill. The maximum value of ΔS for ramp shapes is smaller, about half that for hills (see Hunt *et al.*, 1983). Tentatively, it appears that separation on steep hills may act to limit ΔS_{max} to about unity. The observed reduction in ΔS_{max} below the theoretical result of Jackson and Hunt may also be due, at least in part, to the neglect of the nonlinear inertial terms in their analysis, terms which Britter *et al.* (1981) showed to be substantial even for $h/L_s \simeq 0.4$.

The conical (Fig. 3) and polynomial (not shown) hills show larger speedups than those with larger aspect ratios. This is at first surprising in that calculations by Mason and Sykes (1979) for a ridge and a circular hill, with $h/L_s \simeq 0.45$, $z_0/L_s \simeq 7 \times 10^{-5}$ in our terminology, produced larger speedups for the two-dimensional ridge. However, the extent and significance of the separated region are far greater for the ridge (Castro and Snyder, 1982), and the influence of this region on reducing ΔS is consequently greater than that for the cone. Mason and Sykes obtained $\Delta S \simeq 1.3$ in the field for a circular hill with $h/L_s \simeq 0.45$, whereas the cone and polynomial hills had maxima in ΔS of about 0.88 and 0.95, respectively (with $h/L_s \simeq 1$). The field measurements were made at 2 m, i.e. $z/l \simeq 0.1$, whereas the laboratory measurements were made at $z/l \simeq 1$, so the comparison must be treated with caution.

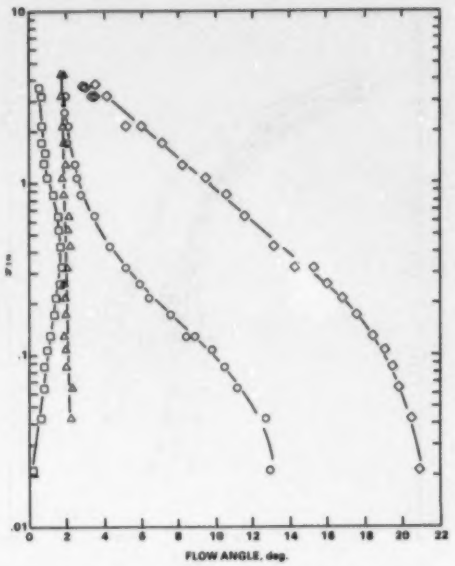

Fig. 5. Angle of mean velocity above hill crests. △, No hill; □, POLY; ○, C2; ◇, CX.

The angle of the mean flow velocity (Fig. 5) above the crest but below 100 mm (0.4h) is the same for C4, C6 and CX, but nearly 10° less for the cone C2 and near zero for the flat-topped polynomial hill. The smaller angles for C2 are an indication of the three-dimensionality and the much-less-deep separated region. At $z/h = 1$, the flow angles are 10°, 6°, 5° and 2° for CX, C6, C4 and C2, respectively, a decrease consistent with an anticipated reduction of flow distortion with height with smaller aspect ratios. The positive flow angle of 2° indicated for flat terrain is possibly indicative of the slow boundary-layer growth, but it is doubtful that the anemometer can resolve flow angles with an accuracy of better than 2°.

The influence of the topography on the streamwise velocity fluctuations $[u' = (\overline{u^2})^{1/2}]$ above the crest is to reduce them below those upstream (Fig. 6). Well above the crest ($z > h$), the variation of u'/U_∞ is determined principally by the different base lines; that is, if absolute height above the tunnel floor were used, the profiles would not be substantially different, as must be the case well removed from the topography. For $z < h$ this is not the case, and the data should be compared on the basis of height above the local terrain. A systematic reduction of u' with increasing aspect ratio is observed, with a maximum reduction of about 30% for the infinite ridge. The polynomial hill (not shown) and the cone results were similar within experimental scatter. Below $z/h = 0.2$, the cone and polynomial hills cause an increase in u' as the surface is approached, a trend

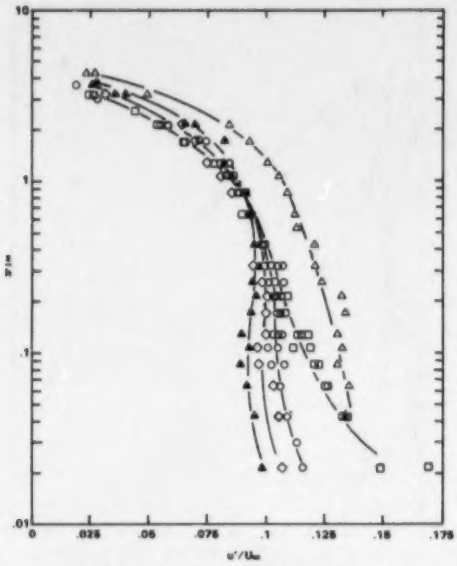

Fig. 6. Streamwise turbulence intensity profiles above crests of hills. △, No hill; □, C2; ○, C4; ◇, C6; ▲, CX.

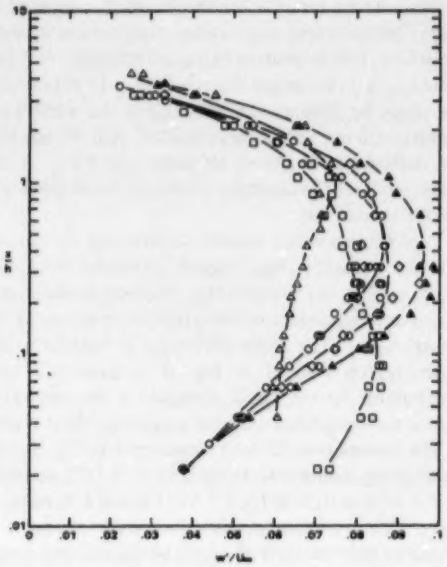

Fig. 7. Normal turbulence intensity profiles above crests of hills. △, No hill; □, C2; ○, C4; ◇, C6; ▲, CX.

not evident for the other hills. The two-dimensional rough hill results (not shown) displayed a reduction in u' similar to the two-dimensional smooth hill except within the lowest 30 mm ($z/h = 0.13$). Within this layer, an increase in u' was observed for the rough hill. Very near the surface (at $z/l = 0.3$ or $z/h = 0.02$), u' for the rough hill was greater than u' over flat terrain.

The normal velocity fluctuations (w') are also strongly affected by the topography (Fig. 7). Well above $z/h = 1.5$, the profiles show essentially little change in w' along a streamline. Near $z/h = 0.25$, a monotonic increase of w' with increasing aspect ratio is observed, with a maximum increase over the no-hill case ranging from about 50% for the infinite ridge to about 25% for the conical hill. The infinite ridge with the rough surface (shown later) produced an increase in w' within the inner region l. The results for the polynomial hill (not shown) were similar to the cone for $z/h \geq 0.35$, then decreased as the surface was approached, in line with C4, C6 and CX, to be the same as the no-hill case when $z/h \sim 0.1$.

The Reynolds stress profiles presented in Fig. 8 show strong effects of the hills. The scatter in the data is rather substantial, but smoothed curves through the data show the general trends. This scatter reflects the uncertainty in measuring the Reynolds stress when the direction of the mean velocity must also be determined. At about half the hill height above the crest, the Reynolds stresses show increases over the no-hill case of approximately 55%. Little difference between the various hills is observed, although a very slight trend of increasing stress with increasing aspect ratio may be discerned. Below about half the hill height, the stresses are dramatically reduced for all hills

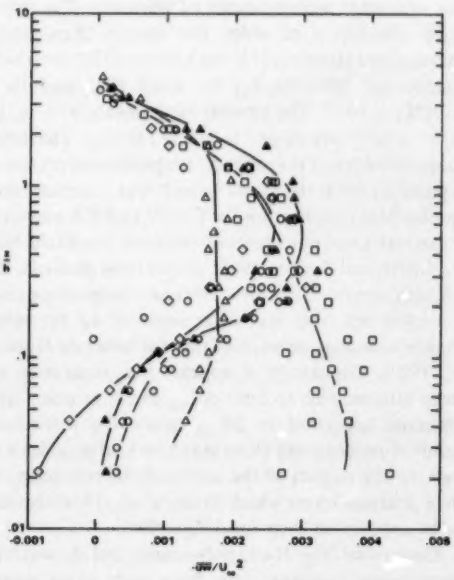

Fig. 8. Reynolds stress profiles above crests of hills. △, No hill; □, C2; ○, C4; ◇, C6; ▲, CX.

except the cone. The stresses near the surface are reduced to very near zero, and there is a hint of a sign reversal. Near the surface above the cone, however, the stresses exhibit dramatic increases, being more than doubled.

How well do these measurements compare with rapid-distortion theory (RDT) and the Jackson–Hunt

(1975) predictions? The latter predictions have been developed for hills of low slope, i.e. small perturbations, but a quantitative comparison will indicate whether they are applicable over a wider range of slopes. RDT applied in the outer region at the crest of a two-dimensional symmetric hill with low slope predicts that (for *isotropic upwind turbulence*)

$$\Delta u'^2/u_0'^2 = -(4/5)\Delta U/U_0, \tag{2}$$

and

$$\Delta w'^2/w_0'^2 = +(4/5)\Delta U/U_0, \tag{3}$$

where ΔU is the velocity change along a streamline and the subscript 0 refers to upstream conditions. The flow over the two-dimensional ridge is not symmetric because of the separation in the lee and because the vortex elements at the crest will have rotated as well as contracted. However, Goldstein and Durbin (1979) show the effect of rotation on u'^2 and w'^2 to be second order in the contraction ratio, and we will neglect effects of rotation here. $\Delta U/U_0$ might be approximated by ΔS, although the former refers to a constant streamline while the latter to constant elevation above the surface. Using this approximation, we note that near the surface $\Delta S_{max} \simeq 0.7$ and so $(\Delta u'^2/u_0'^2)_{max} \simeq -0.56$; this is to be compared with the experimental measurement near the surface of -0.51. The maximum value of $\Delta w'^2/w_0'^2$ was about $+1.1$; however, this occurred at elevations of 0.2–0.4h above the crest, where ΔS had reduced to less than 0.2. These comparisons are based on constant elevation above the surface.

The vertical profiles of mean velocity upstream and at the crest of the ridge were integrated and the stream functions calculated. The horizontal component of the crest velocities was used in the calculation. Interpretation of the data based on streamlines led to essentially the same conclusions as above.

We speculate here that the large values of w'^2 observed are, in part, a consequence of irrotational velocity fluctuations induced by the unsteady wake, which will be most evident in the w' component and should be more evident as the aspect ratio increases.

An observation not initially anticipated was that below about $0.2h$, w'^2 was reduced systematically for all topography except the cone C2 and was equal to that in the upstream boundary layer at about $z/l \simeq 1$ ($z/h \simeq 0.06$). The data for the polynomial hill were broadly consistent with the behavior of C4, although the effect was weaker.

The reduction in w' as the crest is approached may be a result of a reduced influence of the fluctuations in the turbulent wake. Irrotational fluctuations above the crest due to the wake will have a maximum some distance above the crest. The variation with aspect ratio evident in Fig. 7 is consistent with the changes in wake structure observed by Castro and Snyder (1982). In addition, a boundary condition of zero normal velocity will also influence turbulence within an 'eddy size' of a boundary (see Britter *et al.*, 1979; Hunt and Graham, 1978). In the latter paper, grid turbulence near a moving wall (no shear) is influenced by the wall such that the normal component is suppressed, while the other two components are amplified in a region of the order of the turbulent integral scale. The extent of the influence in the normal component extends to about twice that for the other two components.

The results for the cone will be least influenced by an unsteady separated flow (Castro and Snyder, 1982). These results show that the maximum increase in $\Delta w'^2/w_0'^2$ occurs much lower, at $z/h \simeq 0.1$. Comparison with a two-dimensional analysis is inappropriate in this case. However, simple RDT arguments on vortex element stretching lead to a modification of the two-dimensional results. Horizontal vortex elements normal to the flow are stretched as they approach the crest, requiring an increase in u' and w' over the two-dimensional results. This may explain the increase in u' as the surface of the cone is approached (Fig. 6) and the large value of w' near the surface of the cone (Fig. 7). There is little reduction in w' as the crest of the cone C2 is approached, except for a small reduction below $z \cong l$. It also appears that the influence of a rigid underlying surface is (and should be) weakest for the conical hill, since this case has the least nearby underlying surface. The complicated three-dimensional flow near the cone crest will also have an influence on w'.

The data for the cone are in agreement with expectations from RDT arguments applied to the 'outer' region. Although the data for C4, C6 and CX are qualitatively consistent with arguments based on RDT, they may also include contributions from an unsteady separated shear layer. No data were taken, but RDT predicts a second-order (very small) increase in the cross-stream velocity fluctuations for small, two-dimensional contraction ratios and a larger increase when the contraction ratio is not small (the changes in lateral velocity fluctuations are dominated by stretching of longitudinal vorticity).

A comparison of results for the smooth and the rough two-dimensional ridges (Fig. 9a) is interesting. The two profiles are similar throughout the layer except for an increase in w' for the rough surface within the previously estimated inner region of depth l ($= 0.06h$). Because of nearby surface roughness, no boundary-layer data were taken for $z < 2l/3$ (10 mm). However, extrapolation of data for $z \geqslant 2l/3$ to $z = l/3$ gives $\Delta w'^2/w_0'^2 \simeq 1.1$ within the inner region, a significant increase but not as large as the estimate of 4 (h/L_x) provided by Britter *et al.* (1981). Although not presented, u' also increases within l for the rough hill.

The Jackson and Hunt (JH, 1975) theory assumed that the shear stresses were important only close to the wall (in the inner region) and that the flow in the outer region was inviscid and irrotational. Therefore, the relatively large changes in shear stresses in the outer region above the hill crest were unexpected and remain unexplained. This is particularly so for the cone in which little evidence of the fluctuating wake is seen, but a near doubling of the Reynolds stress is observed at $z/h \simeq 0.1$.

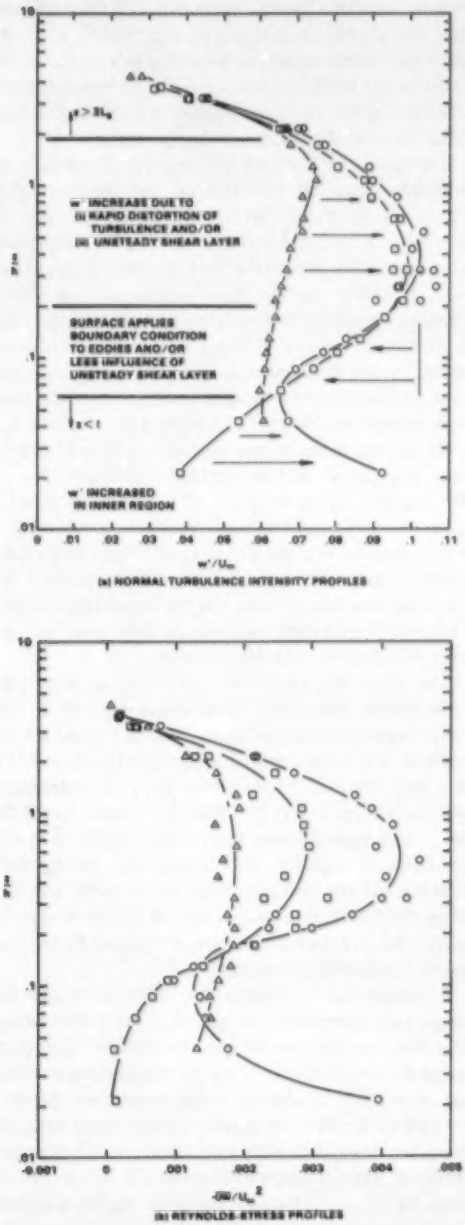
w' INCREASE DUE TO
(i) RAPID DISTORTION OF TURBULENCE AND/OR
(ii) UNSTEADY SHEAR LAYER
SURFACE APPLIES BOUNDARY CONDITION TO EDDIES AND/OR LESS INFLUENCE OF UNSTEADY SHEAR LAYER
w' INCREASED IN INNER REGION
w'/U∞
(a) NORMAL TURBULENCE INTENSITY PROFILES
-uw/U∞²
(b) REYNOLDS-STRESS PROFILES

Fig. 9. Comparison of turbulence parameters above crest of two-dimensional ridge. △, No hill; □, smooth surface; ○, gravel-covered surface. (a) Normal turbulence intensity profiles. (b) Reynolds-stress profiles.

In the inner region, the JH theory predicts very strong increases in the shear stress at the hill crests, e.g. $\Delta\tau_{max} \simeq 5u_*^2$. The observed reductions in stress near the surface for all cases except the cone (which showed an increase by a factor of 2.3) are, at least in part, a result of the reductions in surface roughness over the hills. The JH theory, however, is possibly not applicable because of the large slopes of the present hills. The two-dimensional ridge with a rough surface shows increased shear stresses (Fig. 9b) near the surface when compared with the smooth surface.

JH predicts that the surface shear stress should undergo a small decrease well upstream of the hill, reach a minimum near $x/L_s = -2$, then increase rapidly to a large maximum just upwind of the crest ($x/L_s \cong -0.1$). For the present hills, where the recirculation region is clearly large, the *effective* hill lengths and heights may be greatly increased; that is, the effective hill shape may be more closely related to the hill plus cavity. For example, the two-dimensional ridge exhibited a reattachment point near $8h$ downwind of the crest and a recirculation region perhaps as high as $1.5h$ (see Castro and Snyder, 1982). The effective hill length L_s', then, may have been as large as $4.5h$ (as opposed to $L_s = 1h$ for the actual hill), and the crest of the actual hill would then have been at $x/L_s' \simeq -0.9$. Thus, only small increases in surface stress, u' and w' might be expected.

3.1.2. *Upstream of the hill.* Although upstream flow separations were not observed with flow visualization, the low mean velocities just upstream of the hill resulted in turbulence intensities greater than 30%. Unsatisfactory operation of cross-film probes at these intensities necessitated ignoring turbulence data below $z = 50$ mm ($0.2h$). The mean velocity and angle below this level are suspect but have been included.

Vertical profiles of mean velocity (Fig. 10) show strong reductions in mean velocity close to the ground. C4, C6 and CX are essentially identical, consistent with similar local geometry. At $z/L_s = 1$ ($z/h = 1$), the reductions are monotonic with aspect ratio, reflecting greater

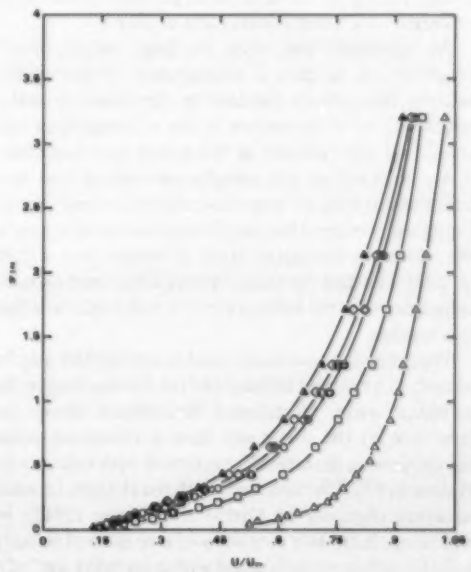

Fig. 10. Mean velocity profiles above upwind bases of hills. △, No hill; □, C2; ○, C4; ◇, C6; ▲, CX.

influence at higher elevations from two-dimensional compared with three-dimensional hills. The relevant speedup factor ΔS near the surface is -0.7, while at $z = L_s$, $\Delta S = -0.28$ for the ridge and changes monotonically to $\Delta S = -0.13$ for the cone. The smooth and rough two-dimensional ridges were indistinguishable down to $z/l \simeq 0.3$.

The variation of flow angle (Fig. 11) is also universal near the surface and dependent upon aspect ratio at height such that the maximum flow angle and the elevation of it increase with increasing aspect ratio.

Just upstream of the hill the streamwise component of turbulence is increased over that for flat terrain (Fig. 12). For the two-dimensional ridge u' is increased by 10% and w' is reduced by 6% for $z/L_s \leqslant 1$. At $z/L_s = 1$, C2 and C4 show an increased w', while C6 and CX are reduced. For u', C2 and C4 are decreased, while C6 and CX are increased. There is order within the data, but the variations are small and confused by scatter. The RDT arguments presented in section 3.1.1 and represented by Equations (2) and (3) indicate that u' should increase and w' should decrease above the upwind bases of the hills. The observations for the ridge are in qualitative agreement with these predictions, but are smaller, particularly near the surface. Stretching of horizontal vortex lines, oriented across the flow, by more three-dimensional shapes C2 and C4 will increase u' and w' and this behavior is apparent in the data of Fig. 12.

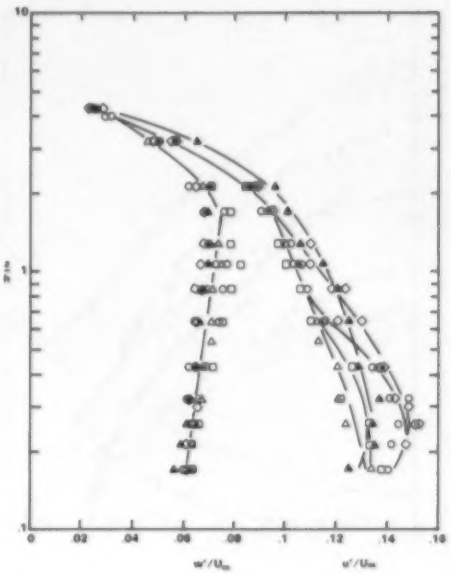

Fig. 12. Turbulence intensity profiles above upwind bases of hills. △, No hill; □, C2; ○, C4; ◇, C6; ▲, CX.

3.2. *Concentration measurements*

For each of the five hills (and in their absence) and for each of the three stack heights, the following concentration profiles were measured:

1. Vertical profiles on the tunnel centerline above the crests of the hills ($x = 3.6h$, $y = 0$; note that x is now referenced to the *source* exit, not hill center).
2. Lateral profiles at the hill crests ($x = 3.6h$, $z = 0$).
3. Lateral profiles above the hill crests through the points of maximum concentration as determined from the vertical profiles ($x = 3.6h$, $z = \text{const.}$), if indeed there was an elevated maximum.
4. Surface profiles on the tunnel centerline ($y = 0$, $z = 0$).

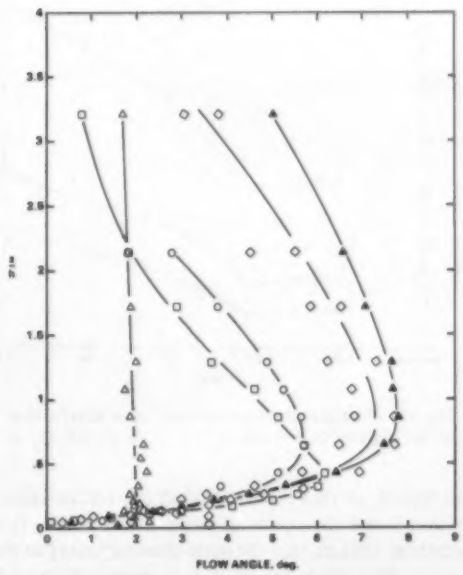

Fig. 11. Angle of mean velocity above upwind bases of hills. △, No hill; □, C2; ○, C4; ◇, C6; ▲, CX.

3.2.1. *Vertical profiles.* To introduce the method of data interpretation we consider the two-dimensional ridge first. Figure 13 shows vertical concentration profiles measured above the ridge crest and at the same position in the absence of the hill. The concentrations are non-dimensionalized as $\chi = CU_\infty h^2/Q$, where C is the fraction of ethylene (by volume) in the sample (above background), h is the hill height, U_∞ is the free-stream velocity, and Q is the volume flow rate of ethylene.

In the absence of the hill, the profiles show elevated maxima very slightly below the release heights and skewed concentration distributions, even when plume reflection from the surface is not evident. The centroids of the distributions will eventually rise, but are little different from the release heights at this position downstream. Above the ridge the maxima are much closer to the surface; the ground-level concentrations (*glcs*) are greatly increased for the elevated stacks (~ 6 times for the stack at half-hill height) and greatly reduced ($\simeq 3$ times) for the ground-level source. The hill has increased the depth of the plume

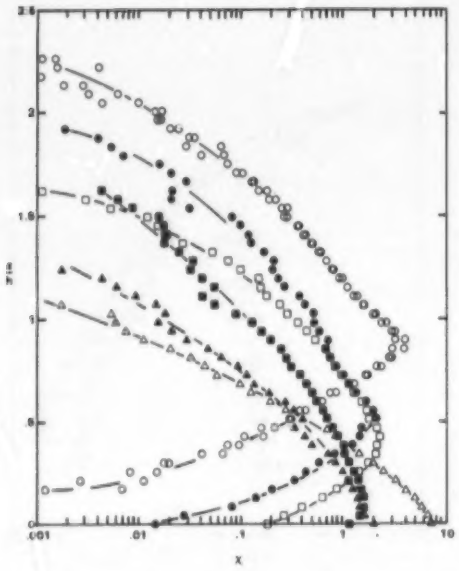

Fig. 13. Vertical concentration profiles above crest of (filled symbols) and in absence of (open symbols) two-dimensional ridge CX. $H_s/h =$: △, 0; □, 0.5; ○, 1.0.

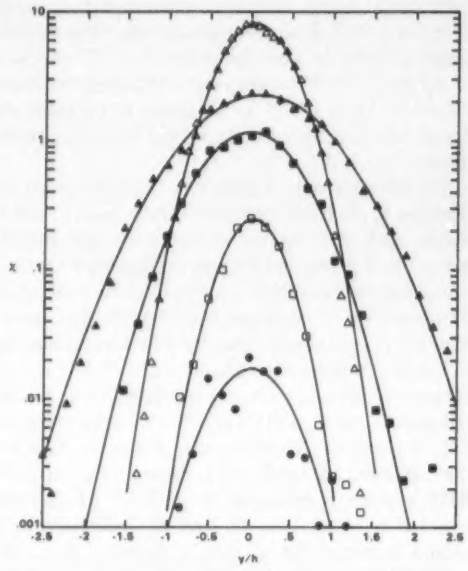

Fig. 14. Surface lateral concentration distributions in presence of (filled symbols) and in absence of (open symbols) two-dimensional ridge CX. Curves represent Gaussian distributions. $H_s/h =$: △, 0; □, 0.5; ○, 1.0.

from the ground-level source, even though the streamlines are contracted substantially going over the crest. That the *glc* from the ground-level source is decreased by the presence of the hill is explained by the substantially reduced transport speed and the excess turbulence spreading the plume. The plume does not appear to converge in the vertical direction; evidently the excess diffusion counteracts the streamline convergence in the vertical, but the lateral spread of the plume is greatly enhanced (Fig. 14). The closer approach of the streamlines to the hilltop and the excess turbulence combine to yield greatly increased *glc*s for the elevated sources. The *glc* due to the hill-height source is increased enormously, but it is still quite small in comparison with that due to the shorter stacks.

We have characterized the vertical concentration profiles at the crest using $\overline{Z}$, the centroid of the vertical distribution, and σ_{zc}, the standard deviation about the centroid. For the ground-level source, $\sigma_z = (\overline{Z}^2 + \sigma_{zc}^2)^{1/2}$ about the surface may be more useful than σ_{zc}. The lateral concentration profiles are quantified in terms of σ_y, the standard deviation about the centroid. In all but a few cases, the lateral profiles are well fitted by Gaussian curves (Fig. 14).

The impact of the terrain on the plumes is most obvious when the centroids of the vertical distributions are compared (Fig. 15). For the elevated sources, the plume centroids above the ridge CX are approximately 2/3 of their upstream heights. As the aspect ratio of the hill decreases, this reduces to about 1/2 for C4 and to about 1/3 for C2 and the polynomial hill. Note that for the polynomial hill, the cone C2, and possibly C4, the plume is considerably convoluted over

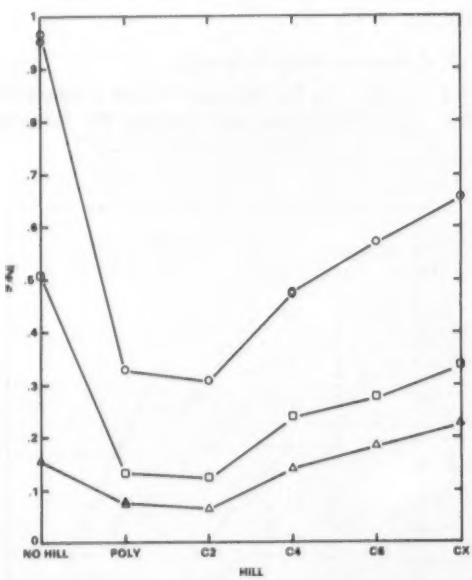

Fig. 15. Centroids of vertical concentration distributions at hill position ($x/h = 3.6$). $H_s/h =$: △, 0; □, 0.5; ○, 1.0.

the hilltop, so that the centroid of the vertical distribution is not the center of mass of the plume. It is apparent, though, that the three-dimensionality of the terrain does allow the plume to approach the hill surface much more closely. The centroids from the ground-level source increase with increasing aspect

ratio such that they are larger over C6 and CX than over flat terrain. As mentioned above, however, because of the convolution of the plume over the hilltop, these centroid values should be interpreted carefully.

For comparison purposes, it would be useful to determine the heights above the crests of the streamlines through the elevated sources. Potential flow theory, for example, may be used to estimate that for $0.3 \leqslant H_s/h \leqslant 1.0$, the streamline through the source (far upwind) passes over the crest of a cylindrical ridge at a vertical distance of $n_s/h = 0.6\,H_s/h$ (within about 10% of potential theory) and over the crest of a hemispherical hill at $n_s/h = 1/3(H_s/h)^2$ (within 3%; for precise formulas, see Egan, 1975). Further, Hunt *et al.* (1978) provided a method for estimating such streamline displacements for arbitrary shapes of ellipsoidal hills. Integration of the mean velocity profiles in the absence of the hills and over the crest of the two-dimensional hill provides experimental data for comparison with the potential flow theory. This comparison, shown in Fig. 16, shows that potential flow underestimates the streamline displacements over the crest of CX by approximately 25%. This may be due to the fact that the effective hill shape is the hill plus cavity, but quantitative comparisons have not been made. Unfortunately, it is not possible to obtain stream functions for the three-dimensional hills. We have also plotted on Fig. 16 the plume centroid values (from Fig. 15) for $H_s = h/2$ and h; they generally vary within the limits suggested by potential flow theory.

The vertical plume widths σ_{zc} (Fig. 17) show similar variations with aspect ratio and stack height as did the centroids $\bar{Z}$. However, it is important to note that for the wider hills and elevated sources, σ_{zc}s are slightly larger than the corresponding flat terrain values,

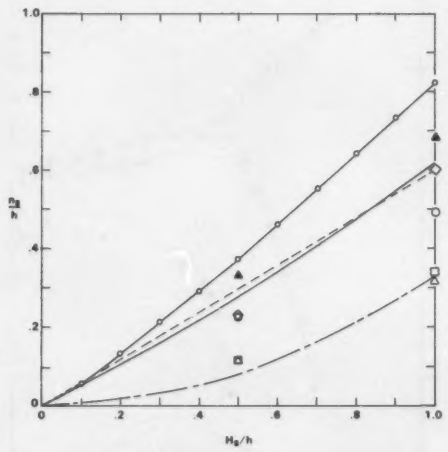

Fig. 16. Displacements of streamlines above crests of hills. Potential flow theory for: ——, cylindrical ridge; – – –, linear approximation for cylindrical ridge; — — —, hemispherical hill. —○—, Determined from integration of mean velocity profiles over CX. Plume centroids for: △, C2; □, POLY; ○, C4; ◇, C6; ▲, CX.

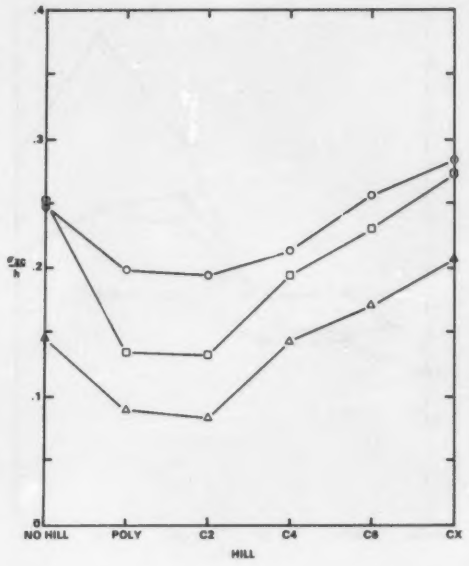

Fig. 17. Standard deviations of vertical concentration distributions over hills. $H_s/h =$: △, 0; □, 0.5; ○, 1.0.

whereas the centroids were substantially smaller than those for flat terrain. For example, for hill C4 and $H_s = h$, the ratio $\bar{Z}/\sigma_{zc} = 2.25$, whereas for flat terrain, $\bar{Z}/\sigma_{zc} = 3.85$. Such a terrain-induced change could lead to a factor of 100 change in hilltop concentration if reflected plume arguments were used. For $H_s = h/2$, the ratio is 1.25 compared with 2.3, which leads to a possible change by a factor of 6 in the hilltop concentration. These estimates ignore changes in lateral plume widths, wind speeds, etc., but they do show that *glc*s are very sensitive to the ratio $\bar{Z}/\sigma_{zc}$.

3.2.2. *Lateral profiles.* The elevated lateral plume widths (through the maxima in the vertical concentration distributions) are increased by the hills, generally increasing with increasing aspect ratio and with decreasing source height (Fig. 18). The plume widths above the two-dimensional ridge may at first appear anomalous, having somewhat smaller values than those for C6. This is readily accounted for, however, when it is realized that σ_y is dependent upon increased travel time, lateral turbulence, and any lateral divergence of streamlines, the last being prohibited in two-dimensional flows. Hanna (1980) also observed a terrain-induced increase in σ_y with field data from a roughly two-dimensional terrain step near the TVA Widows Creek plant.

The lateral plume widths at the hilltops (measured by laterally moving the sampling rake at constant elevation a few mm above the hill crests) are also shown in Fig. 18. Some plume widths are not shown: concentrations were either so small (C4, C6 and CX with $H_s = h$) that a reasonable resolution of the plume width was beyond the capabilities of the hydrocarbon analyzers, or the shapes of the concentration distributions

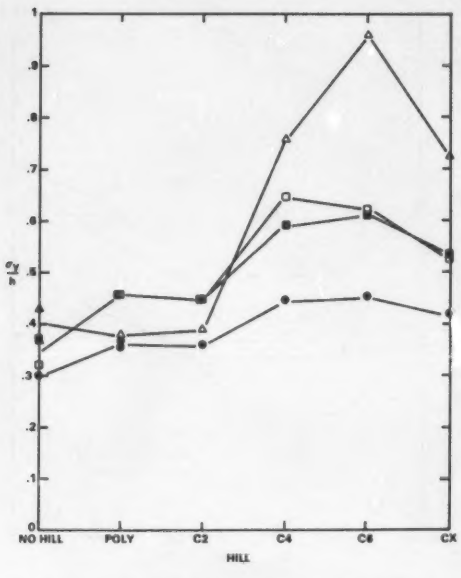

Fig. 18. Lateral plume widths measured at hill crests (open symbols) and at maxima in vertical concentration distributions (filled symbols). $H_s/h =$:△, 0; □, 0.5; ○, 1.0.

were so distorted (POLY, C2 and C4) that a computation of σ_y for comparison with the elevated Gaussian shapes was meaningless. Several important features in the figure are to be noted. First, the hilltop plume widths show generally similar though slightly more pronounced behavior to the elevated widths. Second, in the two-dimensional cases (CX and flat terrain), the hilltop and elevated plume widths are practically identical, which confirms the common assumption in Gaussian diffusion theory of constancy of plume width with elevation. (A more extensive confirmation of this for flat terrain was provided by Khurshudyan *et al.*, 1981.) Third, the plume widths decrease with increases in source height, as is commonly ignored (Irwin, 1979). Fourth, the plume widths for the two-dimensional hill are increased substantially (40–80% increases) over flat terrain, in spite of the fact that the lateral divergence of the streamlines is zero. The excess plume spread is thus evidently due to the increased travel time and the increased turbulence caused by the hill. Now, since the travel times and turbulence intensities are roughly independent of hill shape for C4, C6 and CX (cf. Figs 10 and 11), the increased spread for C4 and C6 over that for CX must be due to the lateral divergence of the flow. The portion of plume spread attributable to streamline divergence is substantial, ranging from 15 to 35%.

3.2.3. *Surface longitudinal profiles.* Longitudinal profiles of ground-level concentration (*glc*) over flat terrain and the various hills are shown in Fig. 19. They display numerous interesting features and, hopefully, clarify some of the effects discussed earlier. First, the profiles over the cone and polynomial hill are quite similar to one another, with concentrations differing generally well within a factor of 2 everywhere. For the half-hill-height source, the location of the maximum concentration is at the crest of the cone, but on the upwind slope of the polynomial hill. Variations of concentration from sources at all three heights are quite smooth.

Second, the profiles over C4, C6 and CX are qu[illegible] similar to one another, but distinctly different from those over C2 and POLY. Abrupt changes in concentrations are observed at the crests of the wider hills.

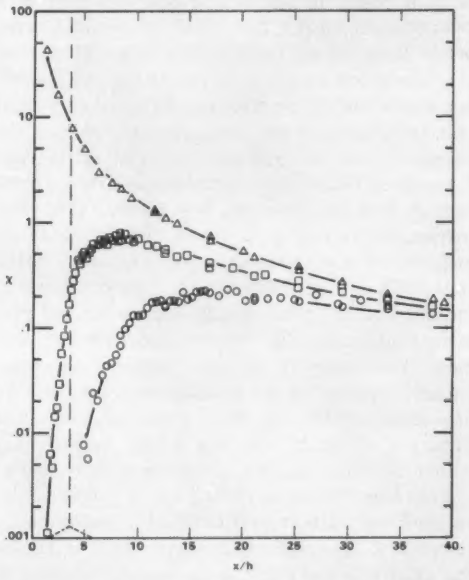

(a) IN ABSENCE OF HILLS.

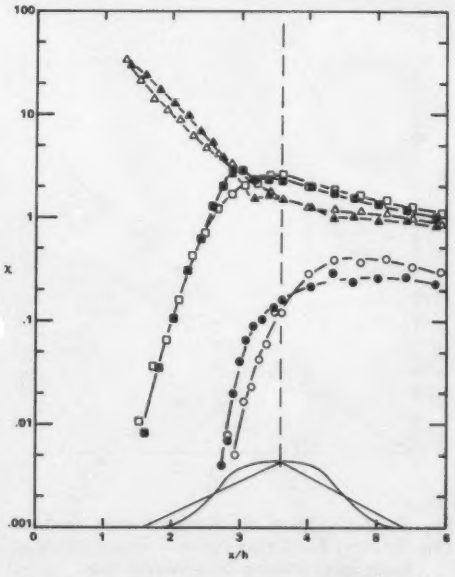

(b) ON CONE (OPEN SYMBOLS) AND POLYNOMIAL HILL (FILLED SYMBOLS).

Fig. 19. (a)–(b).

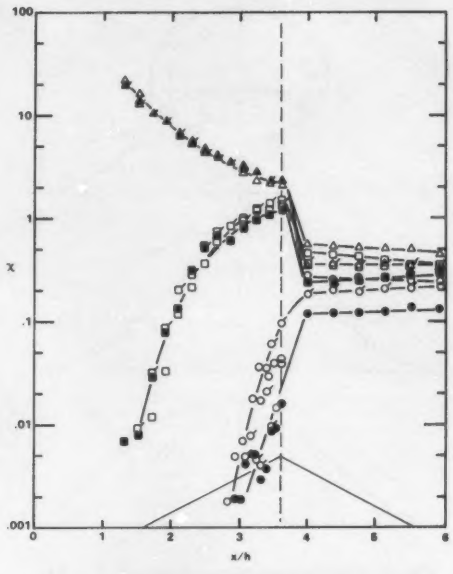

Fig. 19. Surface longitudinal concentration distributions. $H_s/h =$: Δ, 0; □, 0.5; ○, 1.0. (a) In absence of hills. (b) On cone (open symbols) and polynomial hill (filled symbols). (c) On C4 (open symbols), C6, (flagged) and CX (filled).

These jumps are related, of course, to the presence of the large separated/recirculation regions in the lees (Castro and Snyder, 1982). The magnitudes of the jumps range from a factor of 3 (C4) to a factor of 10 (CX), the values presumably related to the size of the recirculation region (Hunt *et al.*, 1979). Note that the jumps are downwards for the two lower sources and upwards for the highest source. For any particular source-hill configuration, the concentration within the recirculation region is effectively constant (along the flow direction but not crosswind, of course), being indicative of the vigorous mixing there.

Third, the locations of the maximum surface concentrations for the elevated sources in flat terrain are well downstream of the hills, whereas in the presence of the hills, the maxima are located on the hill surfaces. For the half-hill-height sources, the maxima are always located at or upstream of the hill crests. For the hill-height sources, the maxima are always located downwind of the crests.

Fourth, for the cone and polynomial hill, concentrations at the crests are larger (by a factor of 2) from the half-hill-height source than they are from the ground-level source. This unusual behavior is evidently explained in that the bulks of the plumes from the ground-level sources diverge around the hills at the lower levels and undergo large dilutions due to the excess surface turbulence, whereas plumes from the half-height sources, while undergoing deformations, essentially engulf the hills, with little excess dilution; the surface concentrations at the crests are essentially identical to plume centerline concentrations in the absence of the hills (cf. Fig. 13).

Finally, and perhaps most importantly, we wish to quantify the effects of the terrain on the maximum *glc* from the elevated sources. This is done through the terrain amplification factor A, defined as the ratio of the maximum *glc* in the presence of a hill to the maximum that occurs from the same source in flat terrain (albeit the maximum may be located in a much different position). These terrain amplification factors are shown in Fig. 20. For the half-hill-height source, all the hills show excess concentrations greater than 40% ($A > 1.4$); the worst case is the polynomial hill, where the maximum surface concentration was 4 times that in flat terrain. The terrain amplification factors for the hill-height source are smaller, ranging from 0.6 to 1.8. These values, especially those for C4, C6 and CX, however, should be treated with caution, because larger concentrations would almost certainly be observed near the reattachment point downstream; unfortunately, measurements were not made in that region. More recent measurements (Thompson and Snyder, 1985) show that for source heights near the hill height, two relative maxima in the surface concentration profile may occur, one near the hilltop and one just downstream of the reattachment point; as the source height is increased within this region the absolute maximum will shift abruptly from the hill surface to near the reattachment point. The region near reattachment was not probed in the present case, so that the terrain amplification factors shown are almost certainly much too small.

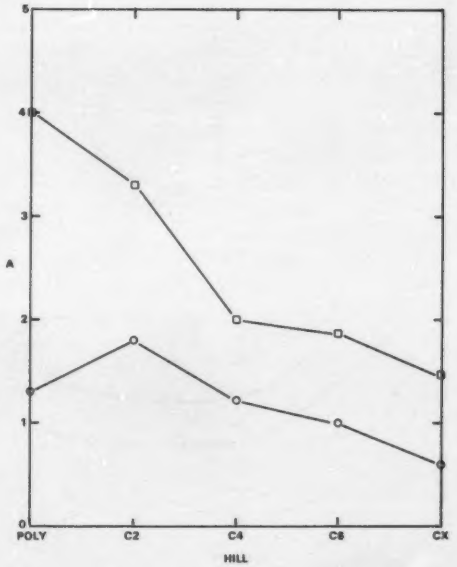

Fig. 20. Terrain amplification factors. $H_s/h =$: □, 0.5; ○, 1.0.

3.2.4. *Detailed examination of polynomial hill.* Lateral profiles at constant (hilltop) elevation are compared with those along the surface of the polynomial hill in Fig. 21. Surface concentration patterns deduced from the surface longitudinal and additional surface profiles taken along the radial lines $\theta = -165°$ and $-90°$ are shown in Fig. 22. The plume shapes sketched in Fig. 23 were deduced from these measurements plus the vertical profiles (not shown).

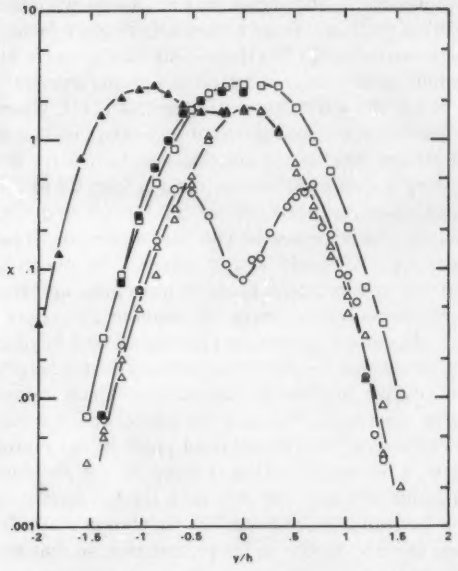

Fig. 21. Lateral (open symbols) and along-surface (filled symbols) concentration distributions over polynomial hill. $H_s/h =$: △, 0; □, 0.5; ○, 1.0.

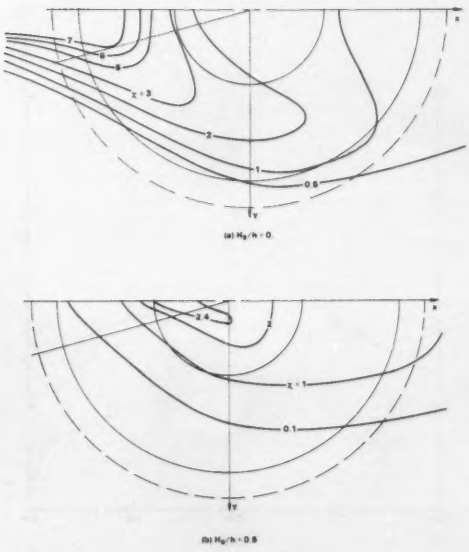

Fig. 22. Surface concentration patterns on polynomial hill. (a) $H_s/h = 0$. (b) $H_s/h = 0.5$.

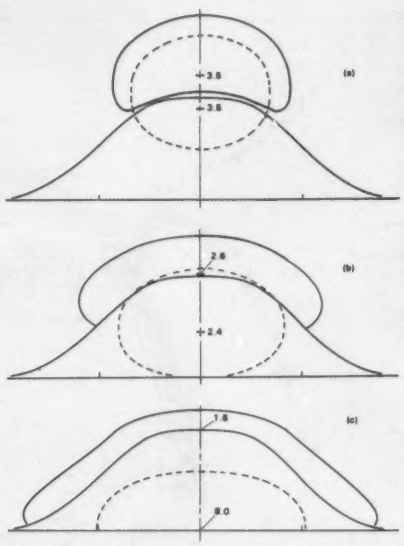

Fig. 23. Plume cross-sectional shapes at $x/h = 3.6$. ——, Over polynomial hill; – – –, in flat terrain. $H_s/h =$: (a) 1.0; (b) 0.5; (c) 0. Contour shown is $\chi = 0.2$. Locations and values of maximum concentrations shown at +'s.

Starting with Fig. 23, plume cross-sectional outlines have been defined as the isoconcentration line where $\chi = 0.2$ (about 10% of the elevated plume centerline concentration in flat terrain; see Fig. 13). The ellipsoidal-shaped plume from the hill-height source in flat terrain is strongly deformed by the hill into a kidney shape, even though the lower edge of the plume has not contacted the hill surface. The lateral profile (Fig. 21) taken at the constant hilltop elevation thus shows a bimodal character, as the sampling tube is below the plume at the hill center and in the wings of the kidney on either side of center.

The plume from the half-hill-height source (Fig. 23), which would have just contacted the flat terrain surface, suffers strong deformations due to the hill, and displays quite large and uniform concentrations over the flat part of the hilltop (Figs 21 and 22). The maximum concentration values are essentially identical to the maximum at the (elevated) plume centerline over flat terrain. The total width of coverage with these large concentrations (within a factor of 2) exceeds one hill height.

The plume from the ground-level source is spread broadly but thinly to cover the entire surface with essentially uniform concentrations (within a factor of 2 out to a radius of $1.8h$ or an elevation of $0.1h$). As mentioned previously, the hilltop concentrations resulting from the half-hill-height source are larger than those from the ground-level source (Fig. 21). However, the hill-*side* concentrations from the ground-level

source exceed those from the half-hill-height source; the maximum surface concentrations on the $-90°$ line are essentially identical for the two sources. The bimodal surface distribution for the ground-level source indicates plume bifurcation (Figs 21 and 22). This bifurcated plume manifests itself simply as a thinner plume over the hilltop and a thicker plume over the sides (Fig. 23). The maximum surface concentration on the 90° line is about 1/3 of the plume centerline concentration in flat terrain; the hilltop concentration is only 1/5 that.

4. SUMMARY AND CONCLUSIONS

The flow fields around moderately steep hills of triangular cross section and varying crosswind aspect ratio and around a bell-shaped hill have been examined using models immersed in a simulated neutral atmospheric boundary layer in a meteorological wind tunnel. The triangular hills ranged from an axisymmetric cone to a two-dimensional ridge. Concentration patterns resulting from sources of three heights placed upwind of each of these hills were examined to determine plume deformations and terrain amplification factors.

The flow field measurements showed similar fractional speedup factors ΔS for the cone and polynomial hill, with a maximum value of about 0.9 at the lowest measuring station of $z/h = 0.04$. The hills with larger aspect ratio showed no obvious trend in ΔS with increasing aspect ratio, but on the whole were substantially smaller than those for the cone and polynomial hill; maximum values again occurred at the lowest measuring station, but ranged from 0.63 to 0.71. The larger speedup factors for the smaller aspect ratio hills were unexpected, but a plausible explanation lies with the separated flow fields; because all the wider aspect ratio hills produced extensive recirculating flow regions in their lees whereas the recirculating regions of the cone and polynomial hill were small or nonexistent, the effective hill shapes (i.e. the hill-plus-recirculating regions) may have appeared more as ramp shapes than crested hills. The ΔS values expected for ramp shapes are about half those for bell-shaped hills. Also, all the speedup factors were considerably smaller than theoretical estimates, both as a result of flow separation and because the theory is invalid for hills of large slope where the nonlinear inertial terms become substantial.

The flow angles at the hill crests increased monotonically with aspect ratio, as anticipated.

Further measurements over a rough-surfaced two-dimensional ridge were generally in good correspondence with the inner and outer regions suggested by Jackson and Hunt (1975). The topographically induced decreases in the streamwise velocity fluctuations and increases in normal velocity fluctuations were broadly consistent with the predictions of rapid-distortion theory in the outer region. However, the large changes in shear stresses in the outer region were unexpected and remain unexplained.

In the region closer to the wall ($z/h < 0.2$), the normal turbulent velocity fluctuations were reduced for all the hills except the cone. These reductions were attributed to the influence of the rigid underlying surface, which was weakest for the cone, and to the influence of the irrotational fluctuations induced by the turbulent wake, which was very small for the cone. The large reductions in shear stresses observed in the inner region were, in part, a result of the roughness change. As above, however, these differences probably also appear because the effective hill shape is more closely related to the hill-plus-recirculation region than to the actual hill shape.

On the flow centerline at the upwind bases of the hills, strong reductions in mean velocity were observed. Whereas the absolute magnitudes of the turbulent velocity fluctuations were not dramatically altered, the local turbulence intensities (i.e. normalized by the local mean velocities) were increased substantially. Hence, plumes transported through this region would be subjected to larger transport times and substantially enhanced dispersion.

The concentration measurements showed strong distortions of the plume shapes effected by the hills. The plume axes approached the hill surfaces much more closely the smaller the aspect ratio. The various types of measurements suggest streamline displacements generally within the limits suggested by potential flow theory.

The convergence of streamlines in vertical planes and divergence in horizontal planes over the hill crests tended to reduce vertical plume widths and increase horizontal plume widths. The increased turbulence intensities upwind of the hills tended to increase both vertical and horizontal plume widths. Over the axisymmetric hills, the net changes in vertical plume width were reductions in the range of 0.5–0.8 times the flat terrain values, showing that streamline convergence dominates over the enhanced turbulence. As the aspect ratio of the hills increased, the streamline convergence was weaker, and the dispersion due to the enhanced turbulence became more dominant. The net changes for the two-dimensional ridge were enlargements in the range of 1.1–1.4 times the flat terrain values. The changes in horizontal plume widths were always positive, ranging from near-zero changes for the axisymmetric hills to over 100% for the ground-level source over C6. In the two-dimensional case, however, horizontal divergence of streamlines was prohibited by the two-dimensionality, so that the horizontal plume dimensions were smaller than those over C6. It should be noted that the horizontal plume dimensions over the axisymmetric hills were not the most appropriate measures; more appropriate dimensions would be the plume widths measured along the hill surfaces, because the plumes generally conformed to the hill shapes.

It is appropriate here to review the three goals presented in section 1, that is

(1) how long (acrosswind) a hill must be to be considered two-dimensional rather than three-dimensional,

(2) how closely a plume from an upwind source approaches a hill surface as a function of the hill's aspect ratio, and

(3) the locations and values of the maximum surface concentrations.

The velocity measurements showed continuous variations with aspect ratio; there were measurable differences on the centerline between C6 and CX. Although systematic variations with aspect ratio were apparent, the differences between C4 and CX were not large by comparison with the differences between C4 and C2.

The concentration patterns also showed continuous variations with aspect ratio. However, concentration patterns on the windward slopes from sources of height 0 and $h/2$ were relatively insensitive to aspect ratio for the wider hills, e.g. maximum surface concentrations for C4 and CX with the half-hill-height source differed by only about 30%; for the ground-level source, the patterns on the windward slopes were essentially identical.

Figure 15 clearly demonstrates how the plume centroids are brought closer to the hill crests as the aspect ratio is decreased.

The longitudinal profiles of surface concentrations showed that for source heights of half the hill heights, maximum concentrations were located at or upwind of the hill crests. For source heights equal to the hill heights, the maxima were always located downstream of the crests. For the axisymmetric hills, larger hilltop concentrations resulted from the half-hill-height source than from the ground-level source. However, hill-*side* concentrations from the ground-level source were considerably larger, essentially equal to those at the crest from the half-hill-height source. Abrupt changes in surface concentrations were observed from the hills of larger aspect ratio due to the flow separation at the crests. The magnitudes of the jumps appeared to be related to the sizes of the recirculation regions. Reductions in concentrations (by factors around 5) occurred for the lower sources, and increases (also by factors around 5) occurred for the highest sources.

Terrain amplification factors A decreased with increasing aspect ratio. For the half-hill-height sources, A values ranged from a maximum of 4 for the polynomial hill down to 1.5 for the two-dimensional ridge. For the hill-height height source, A values ranged from 1.8 for the cone down to 0.6 for the two-dimensional ridge. The A values near and especially those less than 1, however, are suspect, because larger surface concentrations are expected just downwind of the reattachment points but were not measured in the current study. These measurements correlate rather well with those from previous studies as well as with potential-flow arguments suggesting that plumes approach three-dimensional hills more closely than they do two-dimensional ones.

Acknowledgement—REB gratefully acknowledges financial support from the North Carolina State University as a Visiting Associate Professor under Cooperative Agreement Nos. R805595 and R807854 with the U.S. Environmental Protection Agency.

REFERENCES

Arya S. P. S., Shipman M. S. and Courtney L. Y. (1981) An experimental investigation of flow and diffusion in the disturbed boundary layer over a ridge—II. Diffusion from a continuous point source. *Atmospheric Environment* **15,** 1185–1194.

Britter R. E., Hunt J. C. R. and Mumford J. C. (1979) The distortion of turbulence by a circular cylinder. *J. Fluid Mech.* **92,** 269–301.

Britter R. E., Hunt J. C. R. and Richards K. J. (1981) Air flow over a two-dimensional hill: studies of velocity speed-up, roughness effects and turbulence. *Q. Jl. R. Met. Soc.* **107,** 91–110.

Castro I. P. and Snyder W. H. (1982) A wind tunnel study of dispersion from sources downwind of three-dimensional hills. *Atmospheric Environment* **16,** 1869–1887.

Courtney L. Y. (1979) A wind tunnel study of flow and diffusion over a two-dimensional low hill. M.S. thesis, Dept. of Meteorol., NC State Univ., Raleigh, NC.

Egan B. A. (1975) Turbulent diffusion in complex terrain, Workshop on Air Pollut. Met. and Envir. Assess., 30 Sept.–3 Oct., Am. Met. Soc., Boston, MA.

Goldstein M. E. and Durbin P. A. (1979) The effect of finite turbulent spatial scale on the amplification of turbulence by a contracting stream, Unpublished manuscript.

Hanna S. R. (1980) Measured sigma-y and sigma-theta in complex terrain near the TVA Widows Creek Alabama Steam Plant. *Atmospheric Environment* **14,** 401–407.

Hunt J. C. R. and Graham J. M. R. (1978) Free-stream turbulence near plume boundaries. *J. Fluid Mech.* **84,** 209–235.

Hunt J. C. R., Leibovich S. and Lumley J. L. (1983) Prediction methods for the dispersal of atmospheric pollutants in complex terrain. Rpt. No. PPRP-78 to Maryland Power Plant Siting Program by Flow Analysis Associates, Ithaca, NY.

Hunt J. C. R., Puttock J. S. and Snyder W. H. (1979) Turbulent diffusion from a point source in stratified and neutral flows around a three-dimensional hill—I. Diffusion equation analysis. *Atmospheric Environment* **13,** 1227–1239.

Hunt J. C. R. and Snyder W. H. (1980) Experiments on stably and neutrally stratified flow over a model three-dimensional hill. *J. Fluid Mech.* **96,** 671–704.

Hunt J. C. R., Snyder W. H. and Lawson R. E., Jr. (1978) Flow structure and turbulent diffusion around a three-dimensional hill: fluid modeling study on effects of stratification—I. Flow structure. Rpt. No. EPA-600/4-78-041, Envir. Prot. Agcy., Res. Tri. Pk., NC.

Irwin J. S. (1979) Scheme for estimating dispersion parameters as a function of release height. Envir. Prot. Agcy. Rpt. No. EPA-600/4-79-062, Res. Tri. Pk., NC.

Jackson P. S. and Hunt J. C. R. (1975) Turbulent wind flow over a low hill. *Q. Jl. R. Met. Soc.* **101,** 929–955.

Khurshudyan L. H., Snyder W. H. and Nekrasov I. V. (1981) Flow and dispersion of pollutants over two-dimensional hills: summary report on joint Soviet–American study. Envir. Prot. Agcy. Rpt. No. EPA-600/4-81-067, Res. Tri. Pk., NC.

Lawson R. E., Jr. and Britter R. E. (1983) A note on the measurement of transverse velocity fluctuations with heated cylindrical sensors at small mean velocities. *J. Phys. E. Sci. Instrum.* **16,** 563–567.

Mason P. J. and Sykes R. I. (1979) Flow over an isolated hill of moderate slope. *Q. Jl. R. Met. Soc.* **105,** 383–395.

Snyder W. H. (1979) The EPA meteorological wind tunnel: its

design, construction, and operating characteristics. Envir. Prot. Agcy. Rpt. No. EPA-600/4-79-051, Res. Tri. Pk., NC.
Snyder W. H. and Britter R. E. (1979) Sanspray boundary layer characterization. Unpublished Data Report, Fluid Modeling Facility, Envir. Prot. Agcy., Res. Tri. Pk., NC.
Snyder W. H. and Hunt J. C. R. (1984) Turbulent diffusion from a point source in stratified and neutral flows around a three-dimensional hill—II. Laboratory measurements of surface concentrations. *Atmospheric Environment* **18**, 1969–2002.
Thompson R. S. and Snyder W. H. (1985) Dispersion from a source upwind of a three-dimensional hill of moderate slope. Appendix B, EPA Complex Terrain Model Development Fourth Milestone Report—1984, Rpt. No. EPA/600/3-84/110, U.S. Envir. Prot. Agcy., Res. Tri. Pk., NC.

NOTICE

This document has been reviewed in accordance with U.S. Environmental Protection Agency policy and approved for publication. Mention of trade names or commercial products does not constitute endorsement or recommendation for use.

This article documents research that was conducted under the auspices of the U.S. Environmental Protection Agency (USEPA). As an arm of the government, the USEPA has a paid up, non-exclusive, irrevocable, worldwide license to reproduce, prepare derivative works, and distribute to the public all of the material contained herein, and to grant others acting on its behalf the right to do so. The USEPA grants to the National Technical Information Service, Department of Commerce, the right to act as its agent in the distribution of this material.